

Numerical Study of The Effect of Corrugated Wall on The Turbulent Forced Convective Heat Transfer and Fluid Flow Through a Forward-facing Step Channel

Open
Access

Mushtaq Talib Hamzah^{1,*}, Ali Lateef Tarish²

¹ Electromechanical Systems Engineering Department, Thiqar Technical College, Southern Technical University, Iraq

² Department of Thermal Mechanical, Engineering Technical College /Basra, Southern Technical University, Iraq

ARTICLE INFO

ABSTRACT

Article history:

Received 6 November 2019

Received in revised form 9 December 2019

Accepted 10 December 2019

Available online 15 March 2020

Computational analysis of turbulent fluid flow and forced convective heat transfer by forward-facing step with a corrugated wall is performed. The method used for solving the governing equation is the finite element. The SIMPLE algorithm has been useful to study the effect on heat transfer and fluid flow of the Reynolds number (5000 to 2000 range) and the corrugated parameters. The corrugated height and width were (1, 2, 3, 4, and 5 mm) and (10, 15, 20, and 40 mm) respectively. The result observed a significant enhance in the heat transfer by using the corrugated wall and reach up to 50% at corrugated height = 4mm and width = 20mm. Although the rise in the average skin friction coefficient on the same parameter exceeded 53%. Moreover, as the corrugated length and width increase the Nusselt number and skin friction factor increased until reach a particle point and start to decrease again.

Keywords:

Forward-facing step; corrugated; Nusselt number; skin friction; heat transfer

Copyright © 2020 PENERBIT AKADEMIA BARU - All rights reserved

1. Introduction

In the last decades, forward-facing step (FFS) and backwards-facing step (BFS) flow considered one of the most essential areas of research for turbulent convective heat transfer. These types of flows perform an significant character in the development of several engineering applications such as electronic appliances, chemical processes, combustion chambers, heat exchangers, energy system equipment and refrigeration systems.

According to the mixing of low and high fluid resources, the flow isolation and fluid effect in the reattachment zone greatly affect the heat transfer in such systems. This effect depends on the magnitude of the Reynolds number and the thickness of the boundary momentum layer at the step [1]. Because of this, the FFS architecture is more complicated to research than the BFS, where after the step only one recirculation zone is created.

* Corresponding author.

E-mail address: mushtaq.hamza@stu.edu.iq (Mushtaq Talib Hamzah)

The effect of BFS and FFS on the turbulent natural flow convection alongside with a vertical flat plate was experimentally investigated by Abu-Mulaweh [2]. Far step height= 22 mm and a temperature change of 30°C was carried out for the study. The result showed that the maximum Nusselt number obtained in the area of the reattachment zone that was approximately double in the case of BFS and about two and a half in the item of FFS relative to the flat plate rate at identical stream and heat operating conditions. Abu-Mulaweh *et al.*, [3] research the mixed laminar convection flow over a horizontal structure of the FFS applications were performed for Laser-Doppler velocimetry LDV and wire anemometer to measure the reattachment duration for specific inlet velocity and freestream temperature. The results showed that, as long as the flow stays steady, the buoyancy forces related to wall heating have a marginal impact on the temperature distributions and velocity and reattachment distances. Step height and velocity of inlet exhibit a dramatic influence on fluid flow and thermal field. In comparison, with the change in step height and number of Reynolds, the number of the local Nusselt and the recirculation sections decreased upstream and downstream of the step.

The turbulent forced heat transfer was investigated numerically by Yilmaz and Oztop [4] via a double FFS. Study the effect of step length, step height, and number of Reynolds on the fluid flow and heat transfer. A constant temperature applied to the channel's bottom wall while other walls are kept cooler than the bottom wall. The industrial code FLUENT is implemented using the finite-element method. Calculating the flow simulation for double FFS is known to be the standard $k - \epsilon$ turbulence model. The results suggested that both fluid flow and heat transfer can be used as a control tool in the second stage.

Oztop *et al.*, [5] expand the mathematical inquiry on the double FFS by adding a rectangular obstacle before each step of different aspect ratio. This explores the effect of hazard aspect ratio, number of Reynolds, and step height on heat transfer and fluid flow. As the aspect ratio increases, the outcome observed that the pressure drop decreases. In fact, the rate of heat transfer decreases as the obstacle aspect ratio increases and that pattern is affected by the height of step.

Most studies investigating the transfer of heat and fluid flow through FFS considered only the turbulent flow. Nevertheless, Kherbeet *et al.*, [6,7] research the nanofluid flow and heat transfer over micro FFS, both numerically and experimentally.

The effect of different step height and angle of inclination of the duct on the both heat transfer and fluid flow is mathematically examined. Where found in this review, separate step height is 350, 450, and 650 μm . The test revealed that the Nu decreased as the stepping height increased. The angle of inclination of the duct was determined to have no major effect on the fluid flow and heat transfer.

Barman and Dash [8] have recently examined numerically the turbulent flow of fluids and heat transfer over a rectangular channel with a double FFS with cylindrical obstacles placed before each step. The commercial code FLUENT was considered to solve the stander $k - \epsilon$ turbulent model. It studies the implications of different obstacle location ratio and Reynold number on fluid flow and heat transfer. The findings also indicate that the heat transfer factor decreases as the ratio of the obstacle location decreases while the obstacles are placed vertically with the same ratio of location. Other related studied on the BFS and FFS can be found in the literature [9–14]. The turbulent induced convective flow above a forward-facing phase paired with a triangular corrugated wall has not yet been studied, to the best of the authors' data.

The main aim of the current paper is to examine the effect on heat transfer and fluid flow of combined a triangular corrugated wall with an FFS channel. Different corrugation height 1, 2, 3, 4, and 5 mm, corrugation width 10, 15, 20, and 40 mm, and Re in the range 5000 to 20000 are considered. The analysis is provided with the skin friction coefficient and local Nusselt number.

2. Methodology

2.1 Theoretical Model

The current analysis mathematical model and the configuration of the flow are shown in Figure 1. Five separate corrugation height values 1, 2, 3, 4, and 5 mm with four-corrugation width values were considered to investigate the effect of mixing corrugated wall with FFS channel on the fluid flow and heat transfer. Both the inlet and outlet height of the channel are 20 and 10 mm respectively.

The upstream and downstream wall-length was 300 mm to ensure a complete construction area in the inlet and outlet of the channels. All walls regarded as adiabatic walls except 200 mm from the bottom wall adjust to a uniform heat flux= 4000 kW/m². The purified water is used as a fluid and works.

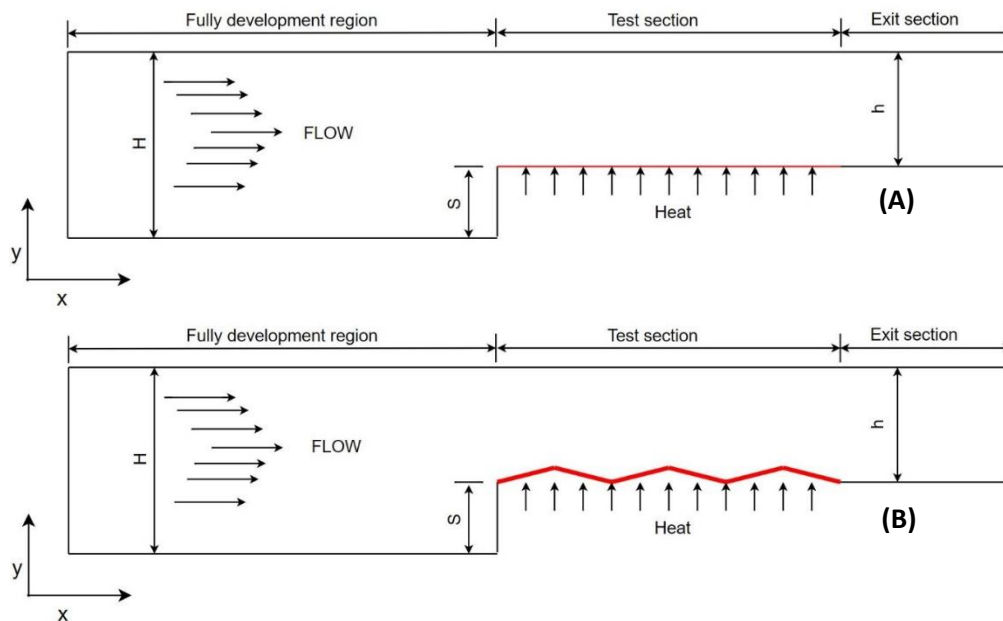


Fig. 1. Schematic diagram of physical problem; (A) forward-facing step channel, (B) Facing step forward associated with corrugated wall.

2.2 Conservation equations

Under the conditions of a Newtonian and incompressible fluid, steady-state flow, 2D, and constant flow the equations of continuity, energy, and momentum are estimated for the case turbulent flow. The conservation equations are written as follows [15];

The equation of continuity:

$$\frac{\partial(\rho\bar{u})}{\partial x} + \frac{\partial(\rho\bar{v})}{\partial y} = 0 \quad (1)$$

The x-Momentum equation:

$$\frac{\partial}{\partial x}(\rho\bar{u}\bar{u}) + \frac{\partial}{\partial y}(\rho\bar{u}\bar{v}) = -\frac{\partial P}{\partial x} + \frac{\partial}{\partial x}\left[(\mu + \mu_t)\frac{\partial\bar{u}}{\partial x}\right] + \frac{\partial}{\partial y}\left[(\mu + \mu_t)\frac{\partial\bar{u}}{\partial y}\right] \quad (2)$$

The y- Momentum equation:

$$\frac{\partial}{\partial x}(\rho \bar{u} \bar{v}) + \frac{\partial}{\partial y}(\rho \bar{v} \bar{v}) = -\frac{\partial P}{\partial x} + \frac{\partial}{\partial x} \left[(\mu + \mu_t) \frac{\partial \bar{v}}{\partial x} \right] + \frac{\partial}{\partial y} \left[(\mu + \mu_t) \frac{\partial \bar{v}}{\partial y} - \frac{2}{3} \rho \frac{\partial k}{\partial y} \right] \quad (3)$$

The conservation of energy equation:

$$\frac{\partial}{\partial x}(\rho \bar{u} T) + \frac{\partial}{\partial y}(\rho \bar{v} T) = \frac{\partial}{\partial x} \left[\left(\frac{k}{C_p} + \frac{\mu_t}{Pr_t} \right) \frac{\partial T}{\partial x} \right] + \frac{\partial}{\partial y} \left[\left(\frac{k}{C_p} + \frac{\mu_t}{Pr_t} \right) \frac{\partial T}{\partial y} \right] \quad (4)$$

where

$$\mu_t = \rho C_\mu f_\mu \left(\frac{k^2}{\varepsilon} \right) \quad (5)$$

At the inlet, section of corrugated wall the boundary conditions taken as:

The inlet velocity equal ($u = u_{in}$) and the velocity at the wall ($V = 0$) and $T_{in} = 300K$

$$k_{in} = \frac{3}{2} (I u_{in})^2, \varepsilon_{in} = C_\mu \frac{3}{4} \frac{K^{3/2}}{L_t} \quad (6)$$

At the outlet, section of corrugated wall the boundary conditions taken as:

$$\frac{\partial k}{\partial x} = \frac{\partial \varepsilon}{\partial x} = 0, \frac{\partial T_f}{\partial x} = 0, \text{ and } \frac{\partial u}{\partial x} = \frac{\partial v}{\partial x} = 0 \quad (7)$$

The wall:

$$u = V = 0, q = q_{corrugated} \quad (8)$$

Heat transfer coefficient

$$h = q \cdot \frac{\ln \left(\frac{T_w - T_{m,in}}{T_w - T_{m,out}} \right)}{(T_w - T_{m,in}) - (T_w - T_{m,out})} \quad (9)$$

$$q = m C_p (T_w - T_{m,out}) / A \quad (10)$$

Inlet velocity

$$u_{in} = \frac{Re \mu}{\rho D_h} \quad (11)$$

The average Nusselt number:

$$Nu = \frac{h D_h}{k} \quad (12)$$

$$D_h = \frac{4A}{p} \quad (13)$$

where D_h , P and A are hydraulic diameter, the channel perimeter and the cross-sectional area respectively.

2.3 Solution Procedure

The numerically calculated and solution of continuity, energy, and momentum using the CFD Ansys FLUENT V.19 based on the finite element method. The $k - \varepsilon$ model with RNG was assumed and the concept of diffusion in the energy and momentum equations was addressed by the discrepancy between the second order and the upwind. The grid is optimized down the bottom wall and for correct tests the scaled velocity and energy residual are set at 10^{-9} . A uniform and non-uniform mesh generations scheme has been adopted in the Figure 2.

Many grid sizes were tested to ensure the exactness and feasibility of the solution scheme. 70,000; 130,000; 270,000; and 400 thousand. Grid size 270,000 has been adopted for the present study depending on the relative error of the result as shown in Table 1.

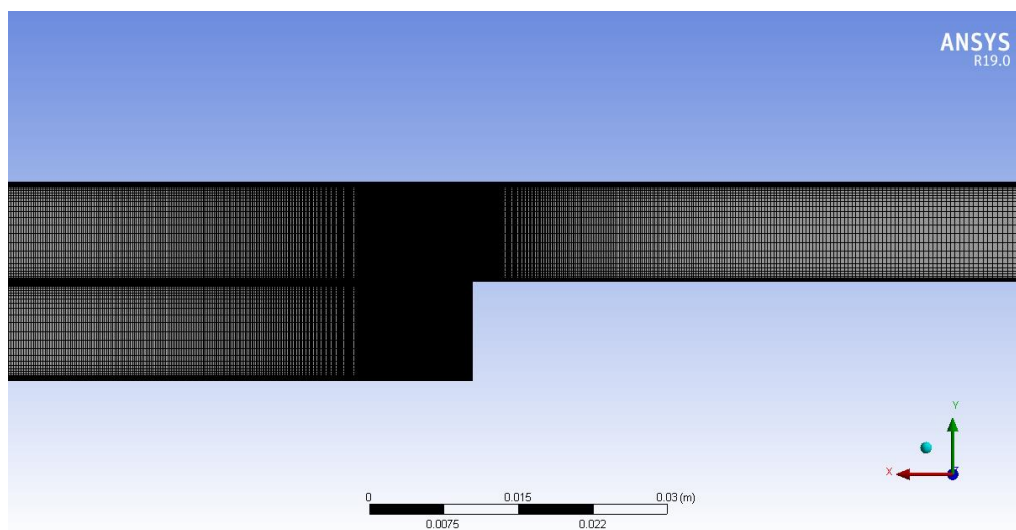


Fig. 2. Micro forward-facing computing grid

Table 1
 Grid independence test

Grid element	Average Nu	e %	C_f	e %
70,000	104.25	-	0.0425	-
130,000	105.95	1.125	0.0395	1.325
270,000	106.12	0.096	0.0354	0.098
400,000	106.52	0.152	0.0332	0.089

2.4 Code Validation

The algorithm is verified by comparing flow and heat transfer data by Hilo *et al.*, [11] over the backward-facing step and Elshafei *et al.*, corrugated channel, [16] with simulated results. The validation for the fluid turbulent flow over a backward-facing step through the average Nusselt number and skin friction factor showed good agreement and is presented in Figure 3.

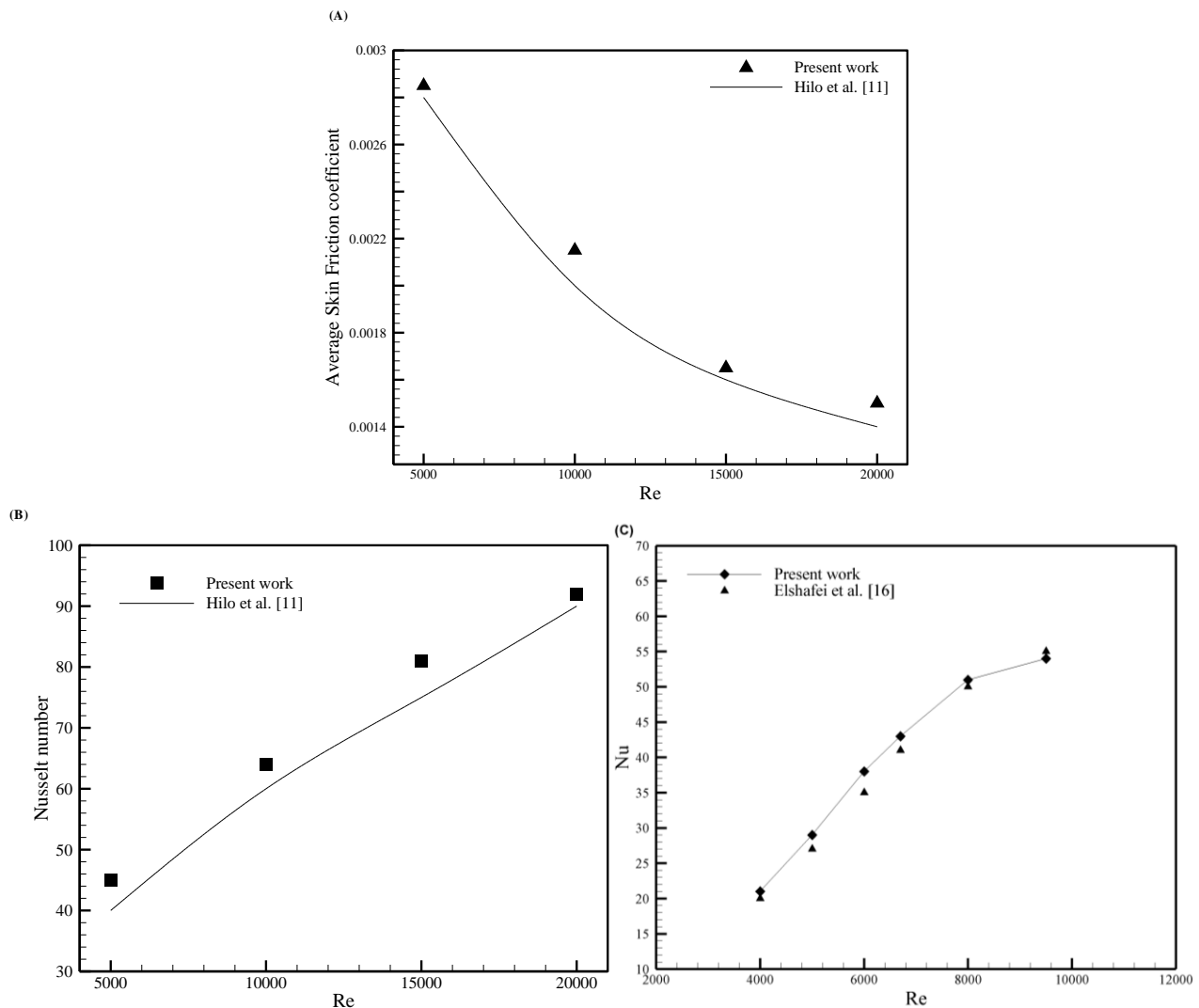


Fig. 3. Validation of the present result of (A) average skin friction and (B) The Nusselt number with the study Hilo *et al.*, [11] (C) Nusselt number Elshafei *et al.*, [16]

3. Result and Discussion

A forward-facing step channel collective with a triangular corrugated wall was considered by the current numerical investigation. The effect on skin friction factor and the Nusselt number of the corrugated wall and the parameter such as corrugation height, corrugation distance, and Reynolds number was discussed. Figure 4 shows the surface Nusselt number along the X-axial direction with different corrugated height at $Re = 5000$. The calculation shown, the rise in Nusselt number decreases with the increase in corrugated height. A significant augmentation in the Nusselt number observed at corrugated height = 5 mm compared to corrugated height = 1 mm. However, the increasing presence in the Nusselt number starts to decline after corrugation height = 3 mm. Moreover, the increase in the Nusselt number could be due to the vortex that generated at each corrugated diverge section and its growth and developed as the corrugated height increase. The pattern of the surface Nusselt number is the same for each corrugated value. The velocity increases in the diverging region, due to a decrease in the thickness of the boundary layer and resulting from finding the highest value of Nusselt number in the diverging segment when the lowest in the coverage region is collected.

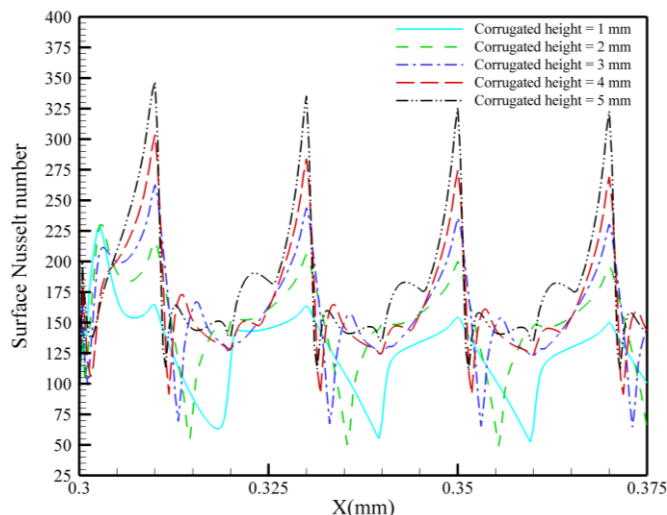


Fig. 4. Surface Nusselt number with different corrugation height at $Re = 5000$

Figure 5 presents the surface Nusselt number along the X-axial with different corrugated width at $Re = 5000$. The surface Nusselt number distribution has the highest value at the first wave and the overall trend of the surface Nusselt number shows an increase as the corrugated width increases. However, this enhancement in the Nusselt number reach the pick at corrugated width = 20 mm and stay to drop after that. This decreasing in the Nusselt number is due to the decreasing the strength of the vortex at the diverging section of each corrugation.

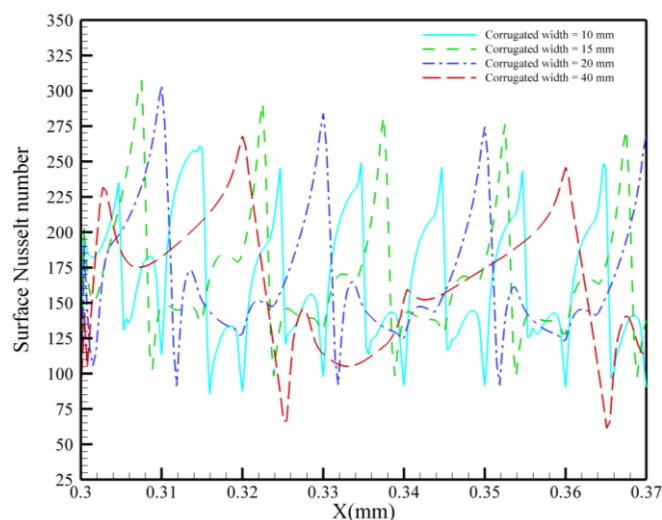


Fig. 5. Surface Nusselt number with different corrugation width at $Re = 5000$

The friction coefficient skin beside corrugated wall of the forward-facing step channel with different corrugated height at $Re = 5000$ is present in Figure 6. The figure shows an increase in skin friction by way of the corrugated height rises. The increasing percentage of skin friction between corrugated height 2, 3, and 4 mm is smaller compared with the one between corrugated height 4 and 5 mm and that may occur as a result of the sharp pressure drop that happens at the corrugation section of 4 and 5 mm. Moreover, the distribution of skin friction shows that the highest and lowest value obtained from the converging and diverging section of the corrugation wall.

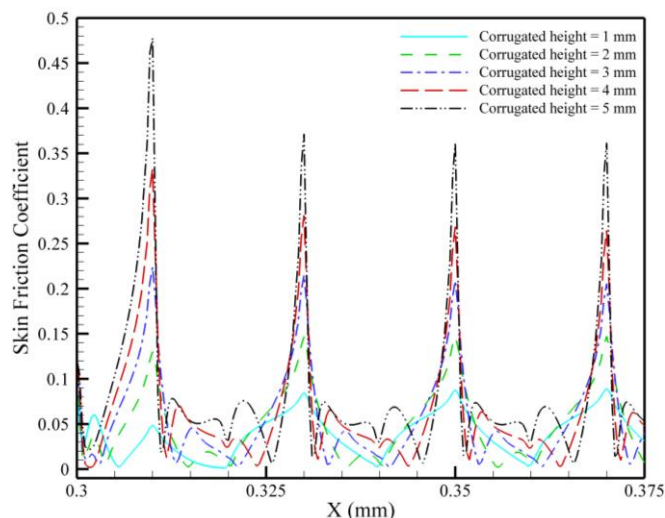


Fig. 6. Skin friction coefficient with different corrugated height at $Re = 5000$

Figure 7 shows the coefficient of skin friction as a variable of the corrugated width (10, 15, 20, and 40 mm), where $Re = 5000$ over FFS channel with a corrugated wall. The effect on the corrugated width on the skin friction increases with the increasing of corrugated width. The skin friction coefficient distribution has the highest value at the first corrugation and took almost the same pattern for all waves at a practical Reynolds number. The maximum increase in the skin friction where observed at corrugated width = 20 mm and it is decreasing at corrugated width = 40 mm.

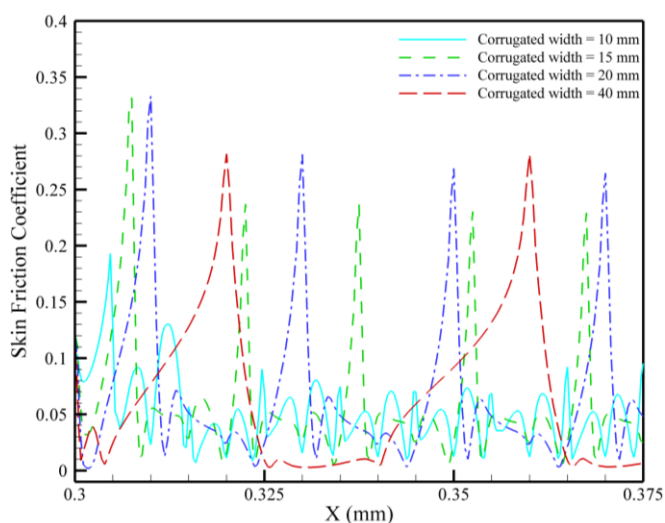


Fig. 7. Skin friction coefficient with different corrugation width at $Re = 5000$

Figure 8 and 9 show the distribution of average Nusselt number and friction coefficient skin for the forward-facing step channel with and without the corrugated wall at the Reynolds number. The enhancement for average Nusselt number and the forward-facing step with a corrugated wall are clear compared to the normal forward-facing channel. As the number of Reynolds increases the number of Nusselt and reduces the skin friction when the number of Nusselt increases where the number of Reynolds decreased for 5000 to 20000. This change in the Nusselt number is due to the increasing size of each corrugated diverge in the recirculation area.

The coefficient of skin friction has the maximum value at $Re = 5000$, and decreases as the Re increases where the coefficient of skin friction is inversely relational with the velocity. Both forward-facing step and corrugation displays a greater coefficient of skin friction relative to the forward-facing step without corrugation.

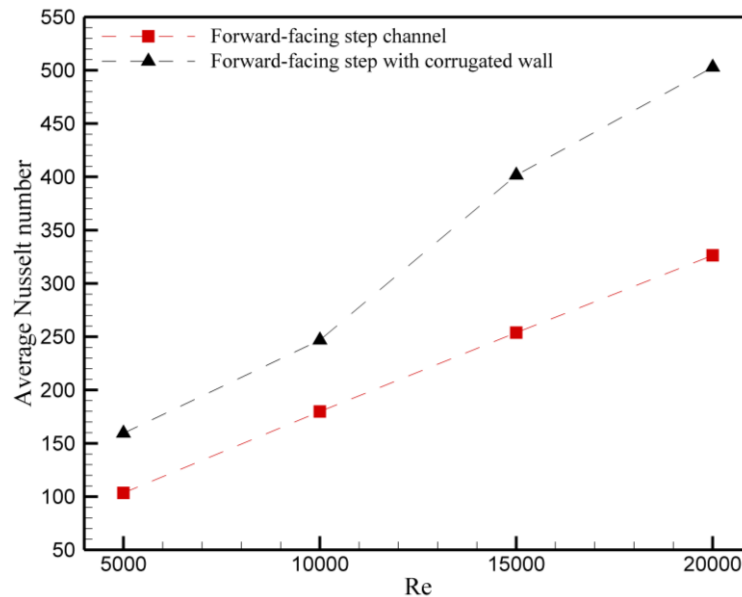


Fig. 8. Average Nusselt number with Reynolds number varies.

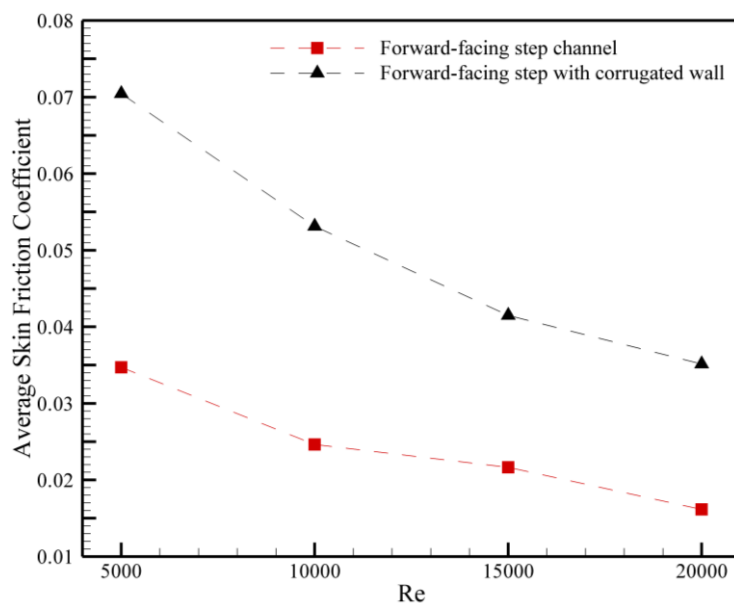


Fig. 9. Differences of Average coefficient of skin friction with Reynolds number

4. Conclusion

In the present paper, both the heat transfer and fluid flow over the FFS channel with and without corrugated walls have been numerically investigated. The effect of the corrugated wall parameter (corrugated height and corrugated width) and Reynold number, Nusselt number and skin friction coefficient are presented. The result shows that integrating the corrugated wall with FFS has significantly improved the Nusselt number with an improvement in the coefficient of skin friction.

Moreover, all parameters of the corrugation wall have affected the heat transfer and fluid flow, whereas the corrugation height and the corrugation width increase the heat transfer increased until reach a specific value. The enhancement of average Nusselt number at corrugated length = 4 mm and width = 20 mm reach approximately 50%. While the increase of average skin friction coefficient reaches 53% at Reynolds number range of 5000 to 2000. The highest value of surface Nu and skin friction coefficient were obtained at the first corrugation of the corrugated surface. Further study on the velocity streamline and the laminar flow characteristics could be extended for future work.

References

- [1] Abu-Mulaweh, H. I. "A review of research on laminar mixed convection flow over backward-and forward-facing steps." *International Journal of Thermal Sciences* 42, no. 9 (2003): 897-909.
- [2] Abu-Mulaweh, H. I. "Effects of backward-and forward-facing steps on turbulent natural convection flow along a vertical flat plate." *International journal of thermal sciences* 41, no. 4 (2002): 376-385.
- [3] Abu-Mulaweh, H. I., Armaly, B. F., and Chen, T. S. "Measurements of turbulent mixed convection flow over a vertical forward-facing step." *Proc. ASME Summer Heat Transf. Conf.* 7, no. 4 (1993): 755-763.
- [4] Öztop, Hakan F. "Turbulence forced convection heat transfer over double forward facing step flow." *International communications in heat and mass transfer* 33, no. 4 (2006): 508-517.
- [5] Oztop, Hakan F., Khudheyer S. Mushatet, and İlker Yılmaz. "Analysis of turbulent flow and heat transfer over a double forward facing step with obstacles." *International Communications in Heat and Mass Transfer* 39, no. 9 (2012): 1395-1403.
- [6] Kherbeet, A. Sh, H. A. Mohammed, Hamdi E. Ahmed, B. H. Salman, Omer A. Alawi, Mohammad Reza Safaei, and M. T. Khazaal. "Mixed convection nanofluid flow over microscale forward-facing step—effect of inclination and step heights." *International Communications in Heat and Mass Transfer* 78 (2016): 145-154.
- [7] Kherbeet, A. Sh, H. A. Mohammed, B. H. Salman, Hamdi E. Ahmed, and Omer A. Alawi. "Experimental and numerical study of nanofluid flow and heat transfer over microscale backward-facing step." *International Journal Heat Mass Trans* 79 (2014): 858-867.
- [8] Barman, Anupam, and Sukanta Kumar Dash. "Effect of obstacle positions for turbulent forced convection heat transfer and fluid flow over a double forward facing step." *International Journal of Thermal Sciences* 134 (2018): 116-128.
- [9] Barbosa-Saldaña, Juan Gabriel, and N. K. Anand. "Flow over a three-dimensional horizontal forward-facing step." *Numerical Heat Transfer, Part A: Applications* 53, no. 1 (2007): 1-17.
- [10] Hattori, Hirofumi, and Yasutaka Nagano. "Investigation of turbulent boundary layer over forward-facing step via direct numerical simulation." *International Journal of Heat and Fluid Flow* 31, no. 3 (2010): 284-294.
- [11] Hilo, Ali Kareem, Abd Rahim Abu Talib, Antonio Acosta Iborra, Mohammed Thariq Hameed Sultan, and Mohd Faisal Abdul Hamid. "Effect of corrugated wall combined with backward-facing step channel on fluid flow and heat transfer." *Energy* (2019): 116294.
- [12] Hilo, Ali, AR Abu Talib, Sadeq R. Nfawa, MT Hameed Sultan, and Mohd Faisal Abdul Hamid. "Review of improvements on heat transfer using nanofluids via corrugated facing step." *Int. J. Eng. Technol* 7 (2018): 160-169.
- [13] Kherbeet, A. Sh, Mohammad Reza Safaei, H. A. Mohammed, B. H. Salman, Hamdi E. Ahmed, Omer A. Alawi, and M. T. Al-Asadi. "Heat transfer and fluid flow over microscale backward and forward facing step: a review." *International Communications in Heat and Mass Transfer* 76 (2016): 237-244.
- [14] Salman, Sadeq, Abd Rahim Abu Talib, Ali Hilo, Sadeq Rashid Nfawa, Mohamed Thariq, Hameed Sultan, and Syamimi Saadon. "Numerical Study on the Turbulent Mixed Convective Heat Transfer over 2D Microscale Backward-Facing Step." 10, no. 10 (2019): 31-45.
- [15] Said, S. A. M., M. A. Habib, H. M. Badr, and S. Anwar. "Turbulent natural convection between inclined isothermal plates." *Computers & fluids* 34, no. 9 (2005): 1025-1039.
- [16] Elshafei, E. A. M., M. M. Awad, E. El-Negiry, and A. G. Ali. "Heat transfer and pressure drop in corrugated channels." *Energy* 35, no. 1 (2010): 101-110.